PALLADIUM(II)-PORPHYRIN COMPLEXES AS EFFICIENT SENSITIZERS FOR SOLAR ENERGY CONVERSION

LIVIU OLTEANU[1,3], RODICA-MARIANA ION[1,2], RALUCA-MARIA STIRBESCU[3], SOFIA TEODORESCU[3], DORIN-DACIAN LET[3], ION VALENTIN GURGU[3], RADU LUCIAN OLTEANU[3]

**Abstract.** The dye-sensitized solar cells (DSSC) and thin-layer heterojunctional solar cells have attracted much attention as an alternative to relatively expensive silicon-based solar cells. Among the various photosensitizers used to build these cells, porphyrins have proven to be outstanding candidates due to their strong absorption in the visible region and have established basic and peripheral modification methods to adjust their geometry and electronic structures. Due to the improved spectral properties, the electronic spectra of these materials have been extensively studied. In this paper, the information obtained using both ultraviolet-visible (UV-VIS) and Fourier Transform Infrared (FTIR) spectroscopy have been used to evaluate the use of Pd-TPP (palladium-5,10,15,20-tetraphenyl porphyrin) as sensitizer dye on different glass substrate coated with transparent conducting oxides. The electrical characterization and quantum efficiency results, related with Pd-TPP-sensitized heterojunctional supramolecular solar cells, are also highlighted.

**Keywords:** metallo-porphyrins; DSSC; Pd-TPP sensitizer dye; UV-VIS; FTIR.

1. INTRODUCTION

The most interesting way to use solar energy is to convert it directly into electricity. Photovoltaic conversion seems to have the greatest potential to become an alternative technology to the classic way of producing electricity in the actual energy crisis [1].

The generation of an electromotive force, under the action of solar energy is the main physical process that underlies the construction technologies of solar cells. The solar cell is a device made from specially treated semiconductor materials, in which, by absorbing light, pairs of electrons and holes are generated, and they are separated spatially due to an internal discontinuity that forms a potential barrier, the electrons being driven in the opposite direction to the holes [2]. The search for clean, cost-effective renewable energy has raised researchers' attention to dye-sensitized solar cells (DSSCs), also known as Grätzel cells [3].

The structure of DSSCs is relatively simple (Fig. 1), the main components being: an anode based on a transparent indium tin oxide (ITO) or fluorine doped tin oxide (FTO) conductor, a layer of TiO_2 or ZnO nanoparticles, an organic dye (organic sensitizers based on ruthenium, with or without metal ions or natural dyes), an electrolyte (the classical electrolyte,

referred to as redox shuttle electrolyte, is the iodide/iodine redox couple, which regenerates the dye ground state by transferring an electron) and a cathode (platinum-based or gold-based, but may be a cathode based on transparent conductors that have a very thin layer of platinum on the surface) [4, 5].
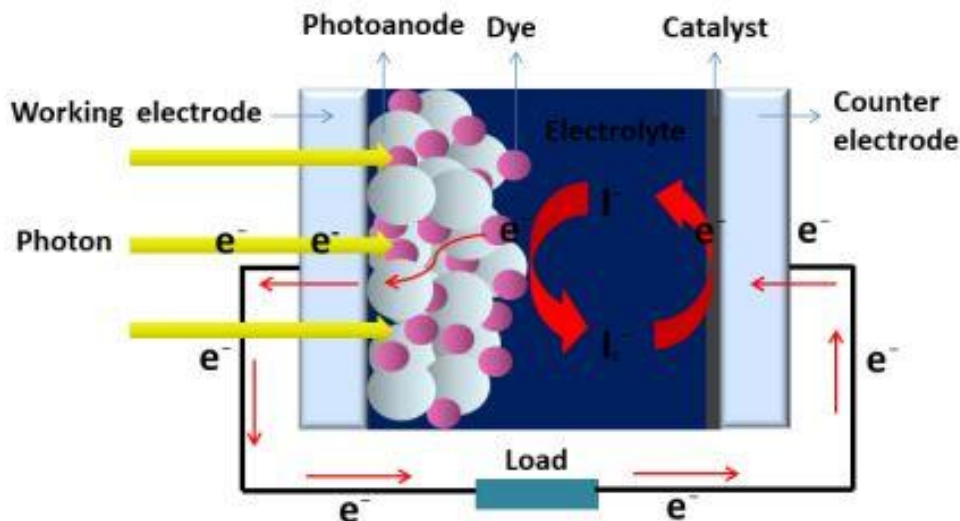

Figure 1. The structure and operating principle of a DSSC [6].

Each of the components in the DSSC has an important role that affects the energy conversion efficiency. The photoexcitation of the sensitizer dye leads to the injection of an electron into the conduction band of the semiconductor. The dye is regenerated by the donation of electrons by the electrolyte (usually a redox system, such as I^-/I^{3-}) in organic solvent. Regeneration of the sensitizer blocks the transfer of electrons back from the valence band to the oxidized dye. The circuit is completed by the migration of electrons. The voltage generated by illumination corresponds to the difference between the Fermi levels of electrons in solid and the redox potential of the electrolyte [7, 8].

DSSCs offer the perspective of low manufacturing costs, without processes that require high energy consumption, high temperatures or high vacuum processes. These cells perform optical adsorption and charge separation process by associating a sensitizer as a light-absorbing material with a broadband semiconductor with mesoporous or nanocrystalline morphology.

The light absorption in the dye monolayer is poor, due to the fact that the total area occupied by a molecule is much larger than the optical section for light absorption. Consequently, a porous, nanostructured film is needed, not a smooth semiconductor surface. When the light penetrates in the semiconductor, it actually intersects hundreds of dyes monolayers. As a result, the semiconductor layer fulfils two roles - dye holder and electric charge collector and current conductor [9].

The conversion of light into electric current is influenced by chemical and physical parameters [10]. Some of the most important characteristics of a photovoltaic cell are: I_{SC} (cell short-circuit electrical current, in A) and V_{OC} (cell open-circuit electrical voltage, in V).

Two other important parameters related to photovoltaic cells are: I_{MP} (current at maximum power, in A) and V_{MP} (voltage at maximum power, in V). These two parameters have been determined by adding to the represented electrical circuit a consumer (resistor), which is connected in series with the ammeter.

Using I_{MP} and V_{MP}, the rated power of the photovoltaic cell, P_{MAX} (in W), was calculated:

$$P_{MAX} = I_{MP} \times V_{MP} \tag{1}$$

The total power of a photovoltaic cell, P_T (in W), was calculated according to the relation:

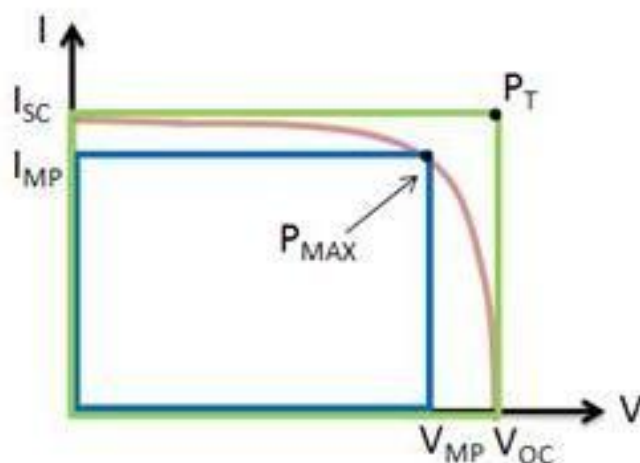$$P_T = I_{SC} \times V_{OC} \tag{2}$$

Figure 2. The electrical parameters of the photovoltaic cells.

The fill factor (FF) and power conversion efficiency (η) were calculated from the following equations:

$$FF = \frac{P_{MAX}}{P_T} \cdot 100 = \frac{I_{MP} \cdot V_{MP}}{I_{SC} \cdot V_{OC}} \cdot 100 \tag{3}$$

$$\eta = \frac{I_{SC} \cdot V_{OC} \cdot FF}{P_I} \cdot 100 \tag{4}$$

where P_I (the power density with photon flux, in W) is the power of light that comes in contact with the photovoltaic cell surface.

In order to be used as a p-type component, the dye must have an absorption spectrum as wide as possible, preferably also in the nearby infrared (IR) zone to collect as many photons as possible. A high extinction coefficient is also required to allow the dye to be used in very thin semiconductor films. At the same time, it must be very tightly attached to the semiconductor surface for greater stability and the energy levels must match the conduction band of the semiconductor and the redox potential of the gap conductor. The synthesis of these compounds must be quite simple for large-scale production and the photostability must be very high in order to be used for at least 20 years.

Porphyrins are a class of naturally occurring pigments, found in biomolecules like: hemoglobin, chlorophyll and cytochrome P450 [11,12]. Porphyrin dyes used in DSSCs are some of the most studied dyes. These compounds present a great interest due to their relatively simple synthesis and the possibility of changing the optical and electronic properties by chemically modifying the porphyrin nucleus [13,14].The reduced performance of these dyes is related to the way of collecting the incident photons, the injection of electrons into the semiconductor oxide (*e.g.*, TiO_2) and the recombination with the acceptor species in the redox mediator.

To remove the collection mode defect of electrons (porphyrin dyes collect very little low-energy photons), they can be used in combination with other dyes [15, 16]. When solving the problems of injecting electrons into the semiconductor oxide, the researchers are looking to change the chemical structure of the dyes so that the transfer is better [17]. Metallo-porphyrins are well known prosthetic groups present in the various proteins and enzymes and they are responsible for the catalytic activities of these biomolecules [18]. In the recent years, metallo-porphyrins have been developed as important synthetic tools for organic transformations [19, 20].

This paper aims to show the involvement of Pd-TPP as a sensitizing dye capable of electronically enriching the sensitizing oxide TiO_2, the realization of DSSC cells, the spectral response of DSSC cells, electrical characterization and quantum efficiency of these cells, as well as the interpretation of the results in accordance with the standards. The porphyrin used is characterized by UV-VIS, FTIR techniques and its photodegradation reaction is monitored.

2. MATERIALS AND METHODS

2.1. MATERIALS

2.1.1. Preparation of 5,10,15,20-tetraphenyl porphyrin (TPP)

A solution of benzaldehyde (20 mmol, 2 mL) in propionic acid (74 mL) refluxed at 170 under air were added drop wise pyrrole (20 mmol, 1.4 mL). After refluxed for 30 min., the reaction mixture washed methanol MeOH (78 ml). The residue was recrystallized with chloroform $CHCl_3$ and MeOH to give TPP.

2.1.2. Preparation OF Pd-TPP

TPP (1.5 mmol, 0.921 g) and palladium(II) acetate (6.0 mmol, 1.34 mg) was dissolved in $CHCl_3$ (123 mL) and refluxed at 90 for 12 h under argon in darkness. Distilled water was added to the reaction mixture and aqueous phase was extracted with $CHCl_3$. The combined organic solution has been washed with saturated aqueous NaCl solution and dried over anhydrous $MgSO_4$, concentrated in vacuo. The residue was purified by flash silica gel column chromatography followed by recrystallization with $CHCl_3$ and MeOH to give Pd-TPP purple solid.

2.1.3. DSSC cells

Three DSSC cells were prepared using a standard procedure [21, 22]. Firstly, the transparent conducting substrates (ITO and FTO respectively) and polydimethylsiloxane (PDMS) with a conductive thin layer of silver (obtained using sputtering technique) were cleaned by treating them with washing powder, ethanol and isopropyl alcohol (IPA). Then, the semiconductor TiO_2 layer was pasted by spin coating technique until a thickness of approximately 25 μm and annealed for 45 minutes in carbolated furnaces at 450°C.

After that, the photo electrodes were dipped in Pd-TPP dye solution in ethanol as solvent overnight. Both working electrode and carbon-coated counter electrode are sealed together using binding clips. Finally, the potassium iodide-based liquid electrolyte was injected in between the electrodes through injection by capillary action.

The schematic workflow for obtaining Pd-TPP dye based DSSC cells and the resulted DSSC cells are presented in Figs. 3 and 4, respectively.
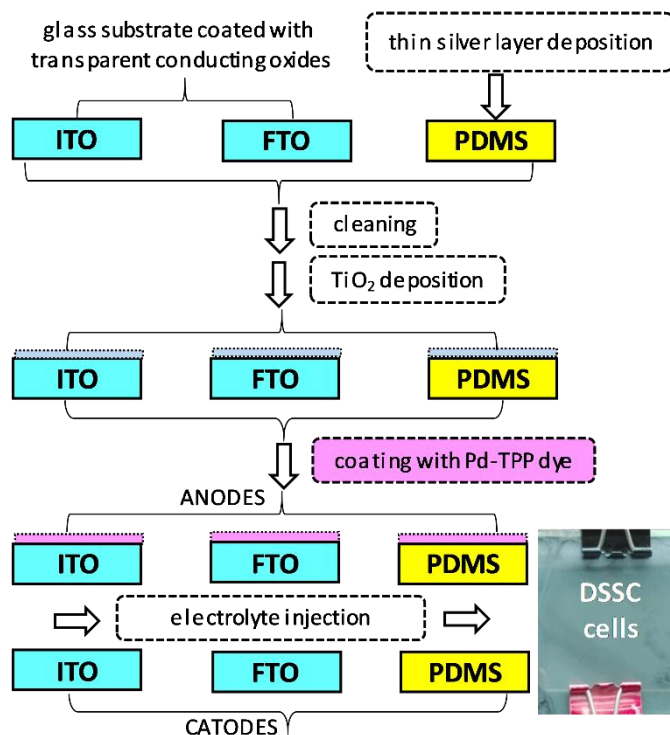

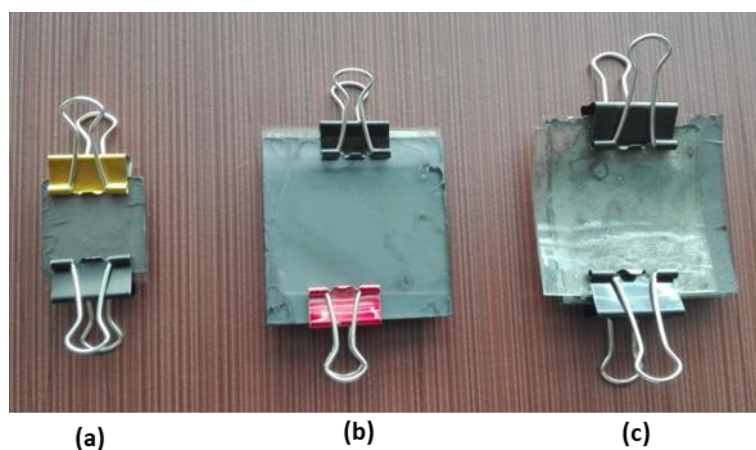**Figure 3. Schematic representation of workflow for obtaining Pd-TPP based DSSC cells**

Figure 4. DSSC cells obtained using Pd-TPP as sensitizer dye on different substrates: a) ITO, b) FTO and c) PDMS coated with silver

2.2. METHODS

The UV–VIS spectra of TPP and Pd-TPP were recorded with a SPECORD M 400 Carl Zeiss Jena spectrophotometer with microprocessor and double beam.

Infrared spectra of TPP and Pd-TPP were measured using an FTIR spectrometer (VERTEX 80), in the following conditions: range 2000 cm^{-1} to 400 cm^{-1}, 32 scan, resolution

4 cm^{-1}. FTIR spectra were achieved using Attenuated Total Reflectance (ATR) accessory with diamond crystal. ATR spectroscopy usually requires little to no sample preparation.

The photobleaching process has been monitored by irradiation with polychromatic light using an Hg-medium pressure lamp of 275 W. The electrical characterization and quantum efficiency of the obtained DSSC cells was performed in the laboratory (*Photovoltaic cells and modules. Testing and characterization*) of ICSTM - Valahia University of Targoviste, Romania.

Investigations regarding the determination of the spectral response and the external and internal quantum efficiency were performed using Newport Oriel IQE-200 equipment. It achieves an accuracy of 0.5 nm in wavelength reproduction with a repeatability of ± 0.2% and a spectral resolution of 10 nm. Newport Oriel IQE-200 is equipped with a 300W Xenon lamp, Cornerstone 130 1/8 m monochromator, Merlin lock-in amplifier and rotating beam obstruction grid.

The measurement of the electrical parameters was performed using the solar simulator Oriel Sol3A, class AAA. The simulator uses a 450W ozone-free lamp containing xenon at 5-20 bar and has a short arc. It reproduces the UV-VIS solar spectrum with dominant xenon lines between 750 and 1000 nm. The simulator has been configured with an AM1.5 global radiation filter that allows the passage of the entire solar spectrum (direct and diffuse) when the sun is at the zenith angle of 48.2°. The equipment is certified according to ASTM E892 standard.

The samples were measured after the solar simulator achieved its nominal operating parameters and the cell surface temperature was reached 25ºC. This was done to comply the IEC 60904-2 standard. The samples were fixed using a vacuum system (min 150 mm Hg). Before measuring the samples, the operating parameters of the simulator (1 sun) were checked using the NIST-certified reference cell based on the ISO-17025 standard. For the measurements performed, the equipment was configured with the necessary filters, and the size of the spot used was 1x1.5 mm.

3. RESULTS AND DISCUSSION

DSSCs are photovoltaic devices which consist of an electrode, an electrolyte and a dye-sensitised photoanode. The efficiency of these systems strongly depends on the photoactive component, i.e., the sensitizer dye. Porphyrins are recognised as potential sensitizers due to their strong absorption bands in the visible region and tunable electronic properties. Until now, the ruthenium sensitizers used as dyes for DSSCs owing to their favourable power conversion efficiency (PCE over 11%) [23].

In a DSSC, a photon is absorbed by the sensitizer (S) leading to the formation of the excited state of the dye (S*). The resulting electron from the valence band of the excited dye (S*) is injected into the conduction band (CB) of the metal oxide. The voltage attainable by the cell corresponds to the difference between the Fermi level of titanium dioxide and the redox potential of the electrolyte. Regeneration of the dye ground state unfortunately limits the attainable open-circuit potential, and this turned out to be a major cause for the relatively low efficiency of DSSCs.

Pd-TPP has a typical absorption spectrum like any metallo-porphyrin with divalent metal (Fig. 5). Pd-TPP shows specific absorption bands: a Soret band at 417 nm (logε = 5.45) and two Q bands at 525 nm (logε = 4.45) and 557 nm (logε = 5.45), respectively.
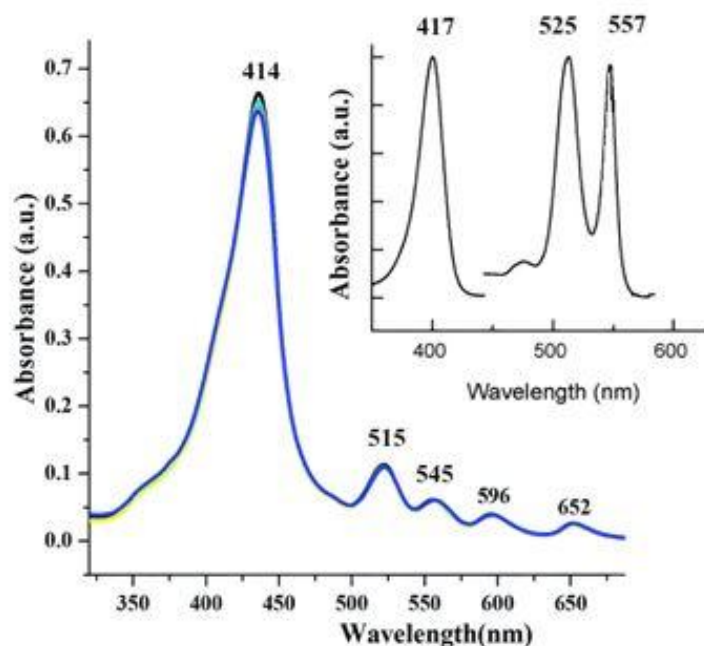
Figure 5. UV-VIS spectra of TPP and Pd-TPP.

The most efficient photosensitizers are those which have strong absorption bands at the infrared range of the visible spectrum an extension of the π-system leads the decrease of the oxidation potential, then the photosensitizer becomes less stable kinetically, thus been subject to photobleaching. In solution, this metallo-porphyrin can remove the metal from the cavity and after that the porphyrin free-base is regenerated, as it can be observed from UV-VIS spectra (Fig. 6).

The Soret band decreases concomitantly with a new band at higher wavelength, while the Q bands disappear and during the irradiation, new bands assigned to free-base species, could be identified. Certainly, new oxidation products could be formed, a first sign being the new bands generated in ultraviolet (UV) region. Based on our previous studies on porphyrins [24-32], these observations suggest that after incorporation into polymeric, ITO or FTO substrates, the metallo-porphyrin stopped its photobleaching reaction, increasing its lifetime for solar energy conversion.
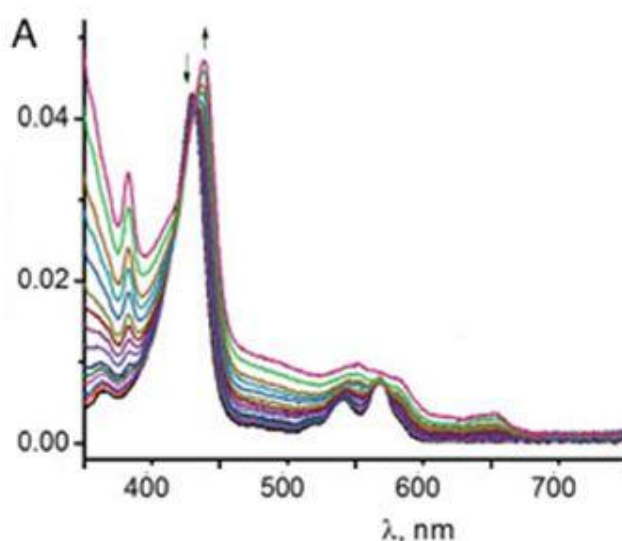

Figure 6. Absorbance decreases during the photobleaching process of Pd-TPP.

From the recorded FTIR spectra (Fig. 7), it was possible to identify the specific bands/spectral features belonging to this new metalloporphyrin by comparison with free-base species, as follows: (1) when the metallic ion was inserted into the porphyrin ring, the N-H bond vibration frequency of free base porphyrins disappeared and the characteristic functional groups of Me-N bond formed at ~1000 cm^{-1}, which indicated the formation of metal porphyrin compounds; (2) the bands at 1494-1682 cm^{-1} and 1334-1352 cm$_{-1}$ were assigned to the C=C stretching mode and the C=N stretching vibration respectively. The bands at ~800 cm^{-1} and ~750 cm^{-1} were respectively assigned to the C-H bond bending vibration of para-substituted phenyl ring; (3) the specific bands for Pd were identified at 555 cm^{-1} (ν Pd–C) and 460 cm^{-1} (ν Pd–N).
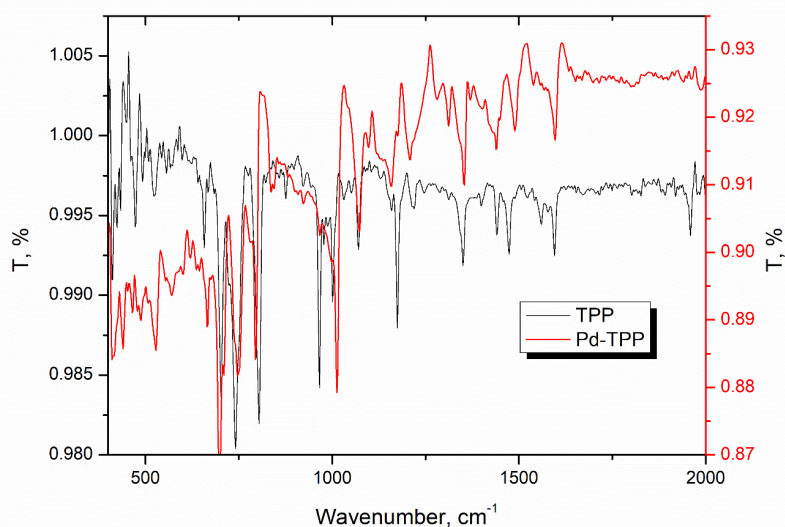

Figure 7. FTIR spectra of TPP and Pd-TPP.

Solar spectral responsivity of the DSSCs depend on the capture of the electrons in TiO$_2$, the lighting conditions, the absorption properties of sensitizer and also, the chemical composition of the cell [33]. The spectral responsivity is determined by measuring the monochromatic incident photon to current conversion efficiency and the image obtained for the three cell types analyzed is shown in Fig. 8.
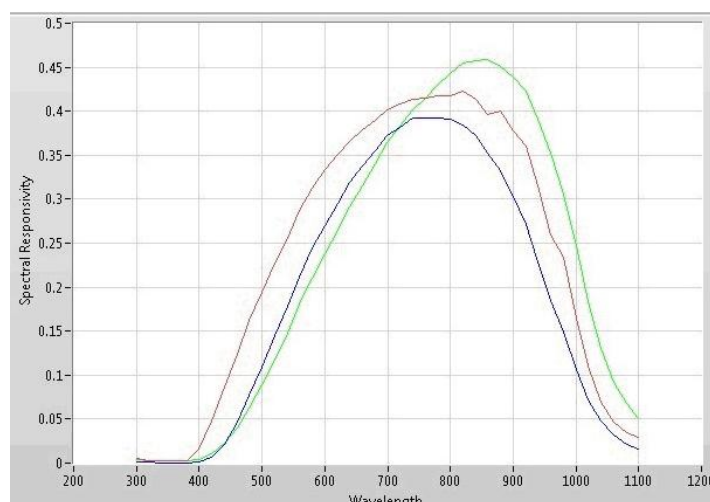

Figure 8. Spectral responsivity for obtained DSSC cells (▬ PDMS, ▬ ITO, ▬ FTO).

Fig. 8 shows that DSSC cell with FTO as transparent conducting substrate give a fast spectral responsivity in comparation with the other two DSSC cells.

The quantum efficiency is conceptually similar to the spectral response. The quantum efficiency gives the number of electrons output by the solar cell compared to the number of photons incident on the device, while the spectral response is the ratio of the current generated by the solar cell to the power incident on the solar cell.

Two types of quantum efficiency of a solar cell are often considered: external quantum efficiency (EQE) is defined as the ratio of the incoming photons, which are transformed to electrons to the external circuit current measurement and internal quantum efficiency (IQE) is defined as the ratio of the number of charge carriers collected by the solar cell to the number of photons of a given energy that shine on the solar cell from outside and are absorbed by the cell [34].
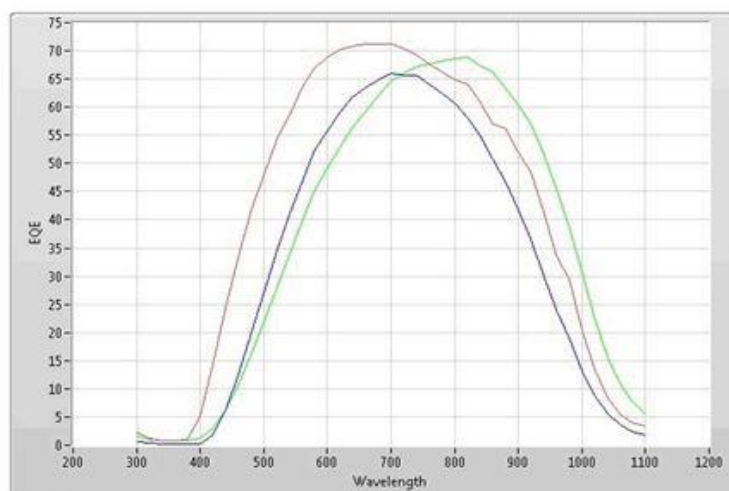

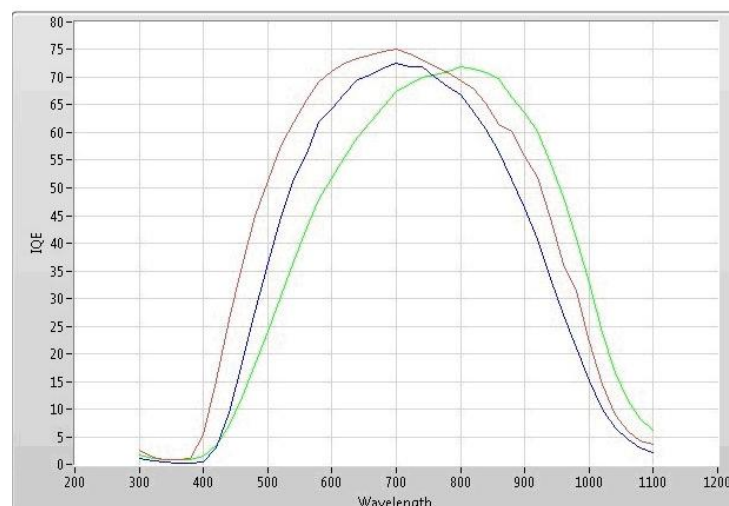**Figure 9. EQE for obtained DSSC cells (▬▬ PDMS, ▬▬ ITO, ▬▬ FTO).**

Figure 10. IQE for obtained DSSC cells (▬▬ PDMS, ▬▬ ITO, ▬▬ FTO).

Figs. 9-10 shows that DSSC cell with ITO as transparent conducting substrate offer a good EQE and IQE relative to the other two DSSC cells.

The current density-voltage (I-V) curves of DSSCs under illumination are used to determine the power-conversion efficiency, η. For the obtained DSSC cells, the I-V curves and the electrical parameters values were shown in Fig. 11 and corresponding the photoelectric parameters were listed in Table 1.
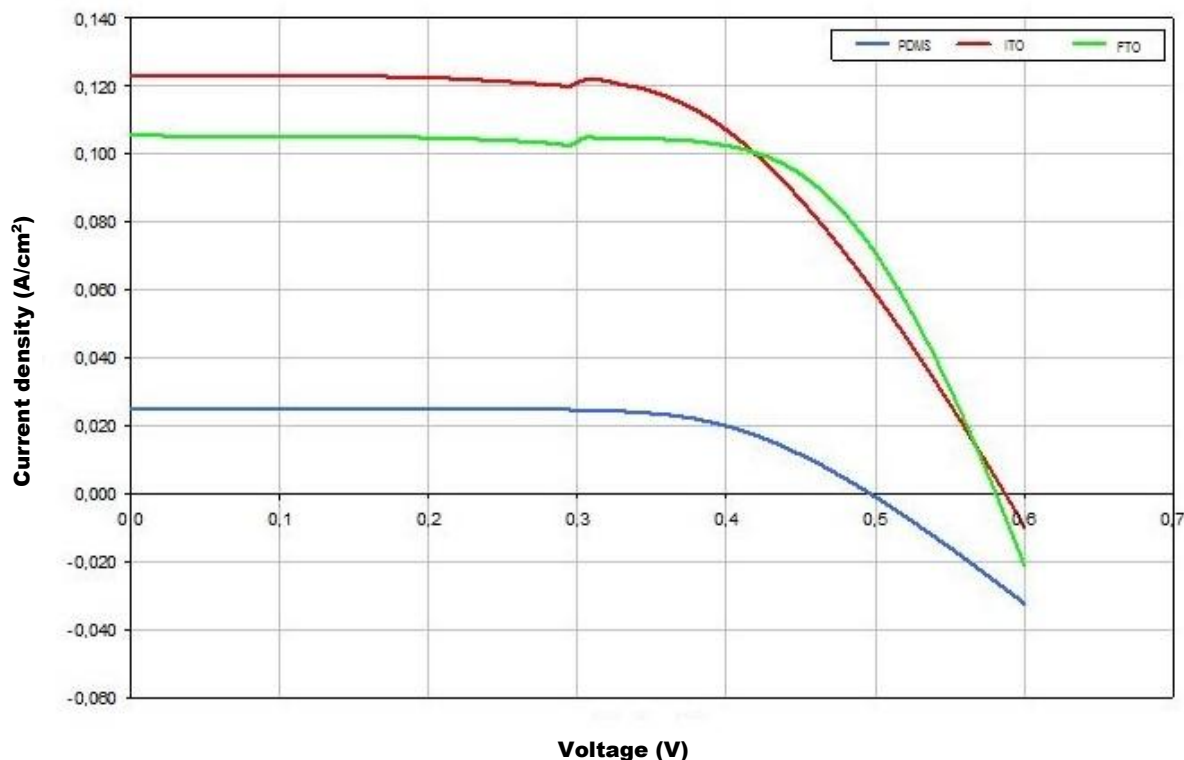
Figure 11. The current density-voltage curves for obtained DSSC cells.

Table 1. Electrical parameters values for the obtained DSSC.

Cell type / conducting substrate	V_{oc} [V]	I_{sc} [A]	I_{max} [A]	V_{max} [V]	FF	η[%]
PDMS	0.4959	0.0252	0.0227	0.3688	**0.67**	**0.35**
ITO	0.5869	0.1230	0.1102	0.3896	**0.59**	**1.71**
FTO	0.5805	0.1054	0.0971	0.4377	**0.69**	**1.70**

From Table 1, the open-circuit voltages (V_{oc}) of these cells showed high values, this being one key parameter in the assessment of the DSSCs performance. Meanwhile, the fill factors (FF) of investigated DSSCs are all higher than 0.4 which indicate that the device shows better conversion capability of photoelectric conversion. Highest efficiency (i.e., 1.70 and 1.71) was obtained for both glass substrates coated with transparent conducting oxides.

4. CONCLUSIONS

In this study, dye-sensitized solar cells performances were investigated for three different transparent conducting substrates: indium-doped tin oxide (ITO), fluorine-doped tin oxide (FTO) and polydimethylsiloxane (PDMS), using the same dye (Pd-TPP), n-type DSSC (TiO$_2$) and electrolyte (potassium iodide-based). FTIR and UV-VIS spectroscopy were used to obtain information regarding the use of Pd-TPP as sensitizer dye in the DSSC assembly.

Analysing the results, we conclude that the most important step in future research is to increase the conversion efficiency of these devices. An innovative solution for transparent conductive materials should be to extend the range of optical transmittance to UV, where photons are much more energetic. Another aspect for future investigations is related to the

improving of the technique of depositing TiO_2 nanoparticles to increase the efficiency of converting light into electricity.

REFERENCES

[1]   Lim, J.H., Leem, J.W., Yu, J.S., *RSC Advances*, **5**, 61284, 2015.

[2]   Bernède, J.C., *Journal of the Chilean Chemical Society*, **53**, 1549, 2008.

[3]   O'Regan, B., Grätzel, M., *Nature*, **353**, 737, 1991.

[4]   Ye, M., Wen, X., Wang, M., Iocozzia, J., Zhang, N., Lin, C., Lin, Z., *Materials Today*, **18**, 155, 2015.

[5]   Klein, M., Pankiewicz, R., Zalas, M., Stampor, W., *Scientific Reports*, **6**, 30077, 2016.

[6]   Jamalullail, N., Smohamad, I., Nnorizan, M., Mahmed, N., *IOP Conf. Series: Materials Science and Engineering*, **374,** 12048, 2018.

[7]   Katoh, R., *Ambio*, **41**(S2), 143, 2012.

[8]   Katoh, R., Furube, A., *Journal of Photochemistry and Photobiology C: Photochemistry Reviews*, **20**, 1, 2014.

[9]   Deepak, T.G, Anjusree, G.S., Thomas S., Arun, T.A., Shantikumar Nair, V., Sreekumaran Nair, A., *RSC Advances*, **4**, 17615, 2014.

[10]   Griffith, M.J., Sunahara, K., Wagner P., Wagner K., Wallace G.G., Officer, D.L., Furube Katoh, A.R., Mori, S., Mozer, A.J., *Chemical Communications*, **48**, 4145, 2012

[11]   Lindsey, J.S., *The Porphyrin Handbook*, Academic Press, San Diego, USA, 45, 2000.

[12]   Milgrom, L.R., *The Colours of Life-An Introduction to the Chemistry of Porphyrins and Related Compounds*, Oxford University Press, New York, USA, 225, 1997.

[13]   Hashimoto, T., Choe, Y.K., Nakano, H., Hirao, K., *The Journal of Physical Chemistry A*, **103**, 1894, 1999

[14]   Griffith, M.J., Mozer, A.J., *Solar Cells - Dye-Sensitized Devices*, InTech, Rijeka, 2011.

[15]   Olteanu L., Ion, R.M., Teodorescu, S., Stirbescu, R.M., *The Annals of "Dunarea de Jos" University of Galati. Fascicle IX, Metallurgy and Materials Science*, **44**(1), 59, 2021.

[16]   Filipič, M., Berginc, M., Smole, F., Topič, M., *Current Applied Physics*, **12**, 238, 2012.

[17]   Sharma, K., Sharma, V., Sharma, S.S., *Nanoscale Research Letters*, **13**, 381, 2018.

[18]   Senge, M.O., MacGowan, S.A., O'Brien, J.M., *Chemical Communications*, **51**, 17031, 2015.

[19]   Olteanu, L., Ion, R.M., Teodorescu, S., Stirbescu, R.M., Dulama, I.D., Bucurica, A.I., *Bulletin of the Transilvania University of Brasov. Engineering Sciences. Series I*, **10**(1), 47, 2017.

[20]   Pandey, V., Jain, D., Pareek, N., Gupta, I., *Inorganica Chimica Acta*, **502**, 119339, 2020.

[21]   Shah, Z.A., Zaib, K., Khalid, M., Saeed, M., *Journal of Fundamentals of Renewable Energy and Applications*, **7**(4), 234, 2017

[22]   Shalini, S., Prasanna, S., Mallick, T.K., Senthilarasu, S., *Renewable & Sustainable Energy Reviews*, **51**, 1306, 2015

[23]   Aghazada, S., Nazeeruddin, M.K., *Inorganics*, **6**(2), 52, 2018.

[24]   Wróbel, D., Hanyz, I., Bartkowiak, R., Ion, R.M., *Journal of Fluorescence*, 8(3), 191, 1998.

[25]   Wróbel, D., Goc, J., Ion, R.M., *Journal of Molecular Structure*, **450**(1-3), 239, 1998.

[26]   Wróbel, D., Boguta, A., Ion, R.M., *International Journal of Photoenergy*, **2**(2), 87, 2000.

[27] Frackowiak, D., Planner, A., Waszkowiak, A., Boguta, A., Ion, R.M., Wiktorowicz, K., *Journal of Photochemistry and Photobiology A: Chemistry*, **141**(2-3), 101, 2001.

[28] Wróbel, D., Boguta, A., Ion, R.M., *Journal of Photochemistry and Photobiology A: Chemistry*, **138**(1), 7, 2001.

[29] Ion, R.M., *Revista de Chimie*, **45**(9), 789, 1994.

[30] Ion, R.M., Tataru, M.S., *Rev. Chim. (Bucharest)*, **44**(9), 736, 1993.

[31] Ion, R.M., Teodorescu, L., Mandravel, C., Volanski, E., Hillebrand, M., *Rev. Chim. (Bucharest)*, **41**(2), 129, 1990.

[32] Teodorescu, L., Ion, R.M., *Rev. Chim. (Bucharest)*, **41**(4), 312, 1990.

[33] Sommeling, P.M., Rieffe, H. C., vanRoosmalen, J.A.M., Schönecker, A.,Kroon, J. M., Wienke, J.A., Hinsch, A., *Solar Energy Materials and Solar Cells*, **62** (4), 399, 2000.

[34] Ananda, W., *Proceedings of the 15th International Conference on Quality in Research (QiR) : International Symposium on Electrical and Computer Engineering*, 450, 2017.